Jordan Journal of Civil Engineering, Volume **2**, No. **2**, **2008**

Study of Soil Compaction Using X-Ray Computed Tomography

O. Al-Hattamleh[1)], M. R. Razavi[2)] and B. Muhunthan[3)]

[1)] Assistant Professor, Civil Engineering Department, The Hashemite University, P.O. Box 150459, Zarqa 13115, Jordan, Tel. +962 (5) 3903333, Ext. 5004, Fax: +962 (5) 3826613, E-mail: hattam@hu.edu.jo (Corresponding Author)
[2)] Assistant Professor, Department of Mineral Engineering, New Mexico Institute of Mining and Technology, 801 Leroy Place, Socorro, NM 87801
[3)] Professor, Department of Civil and Environmental Engineering, Washington State University, Pullman, WA 99164-2910

ABSTRACT

The maximum dry density and optimum moisture content obtained from the laboratory compaction curve have been used customarily to characterize the field behavior of compacted soils. It is well known, however, that the microstructure of compacted soils is dependent on the method of compaction. The structure has an important influence on the engineering behavior of compacted soils. Therefore, in order to provide a better description of compacted soils, methods that can quantify the changes in microstructure are needed. In this study, compacted specimens at various densities and water content were scanned using X-ray Computed Tomography (CT). It has been found that there is direct correspondence between the CT numbers, soil dry density and moisture content. The scanning observations showed also the development of shear planes parallel to the surface of the compacted soil, and changes in structure of the soil towards a more uniform arrangement around the point of optimum moisture content. Compaction of the soil beyond the optimum moisture content appears to disperse soil particles with an overall uniform structure.

KEYWORDS: Computed tomography, Compaction, Dry density, Moisture content, CT numbers, X-ray.

INTRODUCTION

Compaction has been one of the most important methods of ground modification. The compaction process is achieved through many methods such as shallow compaction, dynamic deep compaction, blasting, water jetting, … etc. The result will be the increase of the soil dry density regardless the object, which might be the increase of the shear strength and bearing capacity or the reduction of compressibility, permeability and liquefaction potential which controls swelling, shrinking and prolongs durability (Ingles and Metcalf, 1973; Hausmann, 1990; Rowe, 2000).

The understanding of compaction process traced back to the work of Proctor (1933). Proctor hypothesis states that in low water content, because of capillarity and surface tension, the compaction is difficult. Adding water reduces the capillarity forces and water decreases the friction and acts as a lubricant. The lubricant affects to rearrange the particles until the moisture becomes just sufficient to fill almost all the voids whilst the soil has the greatest density and the lowest void ratio. If more water is added, the soil softens and the dry density reduces. This theory was related to the time when the concepts of effective stress and pore water pressure were not widely known; so it is no longer considered appropriate.

Hogentogler (1936) expanded the lubrication effects

Accepted for Publication on 1/4/2008.

by considering four stages of wetting process in the compaction curve including hydration, lubrication, swelling and saturation, respectively as moisture content increases. Buchanan (1942) proposed a similar theory to Proctor in which he explained soil compaction by considering arch action of soil particles. Hilf (1956) applied the concept of pore water pressures and pore air pressures to examine the compaction curve. Olson (1963) studied air permeability and considered negative residual pore pressures in his theory. He paid attention to a dramatic decrease in air permeability beyond the optimum water content. Lambe (1958) proposed a theory of physicochemical interaction of clay particles by optical examination of the microstructure of clay, however, it may not explain the compaction curve. Leflaive and Schaeffner (1980) proposed to use the air permeability as a criterion to evaluate the compactibility of soils. Whyte and Vakalis (1987) related the compaction to shear surfaces induced by the process. Moreover, McDonald (1988) examined the formation of shear planes parallel to the surface of the compacted soil (pan caking) by discussing the paper of Sherard et al. (1984).

Table 1: Properties of Soils A and B.

Soil	*Description*	*USCS*	G_s	*LL %*	*PL %*	*PI %*
A	Silty Clay	CL	2.67	46	27	19
B	Kaolinite	CH	2.69	64	36	28

Table 2: Properties of Soil C.

Soil	*Description*	*USCS*	C_u	C_c	G_s	e_{max}	e_{min}	ρ_{min}, kg/m^3	ρ_{max}, kg/m^3
C	Silica Sand	SP	2.17	0.75	2.65	0.76	0.56	1531	1786

X-ray computed tomography has been used to determine the bulk density of soil samples by many researchers (Petrovic et al., 1982; Tollner, 1984; Bresson and Moran, 1998; Rogasic et al., 1999). The scope of the above mentioned studies was to quantitatively determine the bulk density of the soil samples and relate the X-ray absorption to soil water content. None of those studies was dedicated to examine the progression of soil compaction curve. In this paper, soil compaction and the confirmation of the proposed compaction theories using X-Ray Computed Tomography were discussed.

X-RAY COMPUTED TOMOGRAPHY

X-ray computed tomography has a great potential to be used for determining the compaction level (i.e., soil bulk density, its 3-D variation and water content). Computed Tomography (CT) imaging is also known as "CAT scanning" (Computed Axial Tomography). CT provides images, which show the density distribution of the material. Three-dimensional images with incredible resolution can be obtained by reconstruction of CT raw images. Details of the particles as well as void characteristics and their distribution can be obtained from CT images, without destroying or disturbing the specimen. Each color or grey shade in CT images is related to a specific CT number. CT numbers are proportional to attenuation coefficients of the material.

In this study, the CT scans were performed at the Washington State University High Resolution X-Ray Tomography facility (WAXCT). The facility consists of Flat panel amorphous silicon high-resolution computed Tomography or FlashCT. FlashCT is an advanced high-speed, industrial, X-ray based 3-D scanning system for nondestructive testing and evaluation. FlashCT is suitable for use within a wide spectrum of X-ray energies and geometric magnifications. Washington State University's

FCT-4200 is a novel design that incorporates both an X-tek 225 keV micro-focus X-ray source for material characterization at high magnification and a Pantak/Seifert 420 keV X-ray source for larger component analysis housed in a single radiation cabinet enclosure. The detector employed is a Varian PaxScan 2520 with CsI scintillator. With the wide energy spectrum and high magnification available, the FCT-4200 can image a large variety of sample shapes, sizes and densities.

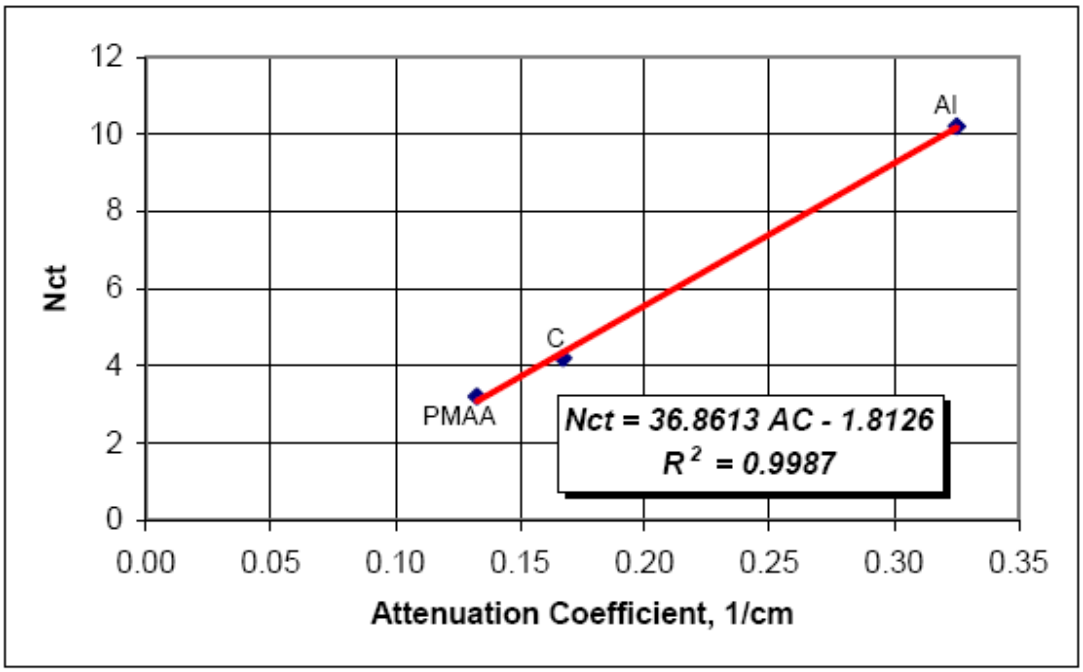

Figure (1): Relationship between the attenuation coefficients of standard specimens and their average CT numbers.

Soil Description

The tests reported in this paper were conducted on three types of soil. The first soil is a local soil from Pullman, Washington, USA designated by soil A. The other two soil types are kaolinite soil, and Silica 30-40 sand, marketed by ECC International and U.S. Silica Company, respectively and designated soils B and C. The properties of those soils have been summarized in Tables 1 and 2.

MECHANICAL COMPACTION TESTS AND CT SCANNING

A series of compaction tests were performed to obtain the compaction curve for both soils A and B. The compaction tests were conducted according to ASTM D 4609-01, Annex A1 (2004) using Harvard miniature apparatus. A portion of the soil passing the No. 4 (4760-micron) sieve was used for compaction. The soil was compacted in five layers in the mold using 25 files per layer. A tamping force of about 40-lb was applied, and tamps were applied at an approximate rate of 10 tamps per 15 seconds. Each compacted specimen was extruded and scanned using the micro-focus 225 keV X-ray tube. The energy level and current intensity of 197 keV and 117μA, respectively were used to scan the specimens with a spatial resolution of 17 μm.

DENSITY CALIBRATION OF COMPUTED TOMOGRAPHY DATA

Density calibration was done according to ASTM-E

1935-97 (2003). Three small cylindrical specimens of aluminum, carbon and PMAA ($(C_5H_8O_2)_n$), which is a special polymer, were scanned as standard specimens for density calibration. The attenuation coefficients for the aluminum, carbon, hydrogen and oxygen were obtained from NIST (National Institute of Standard and Technology) web site (Seltzer and Hubbel, 1995). Figure 1 shows the relationship between the attenuation coefficients of standard specimens and their average CT numbers. This figure is used to compute the density of the soil and its three-dimensional variation.

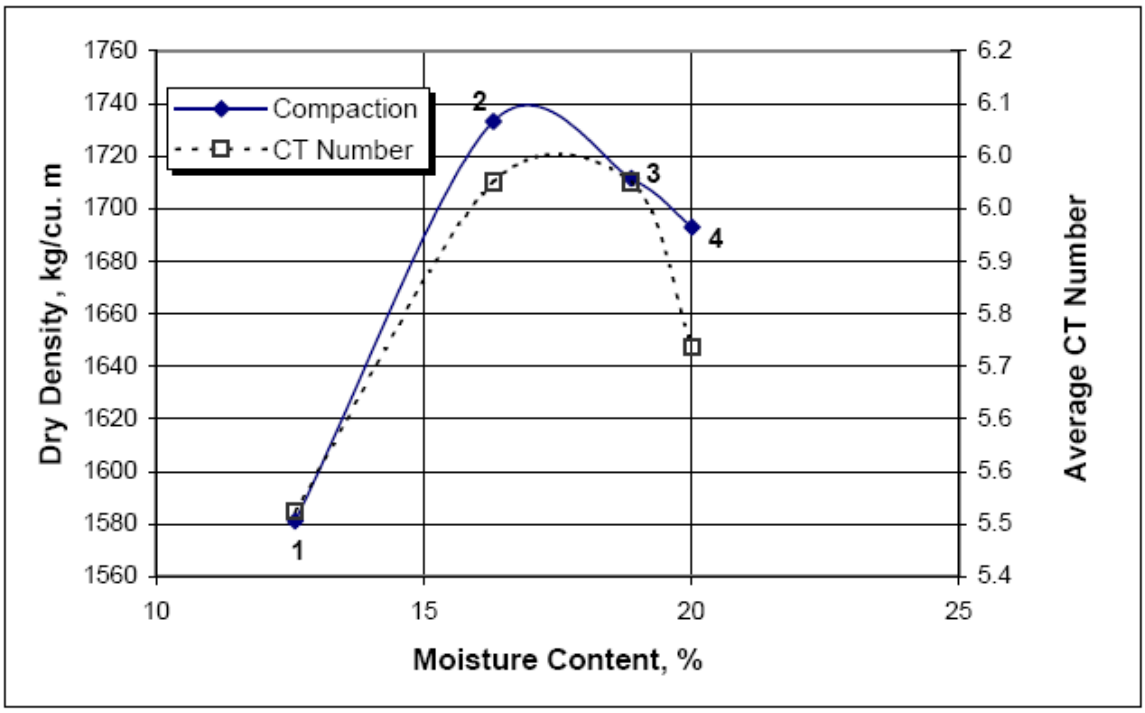

Figure (2): Compaction curve and CT numbers (soil A).

RESULTS AND DISCUSSION

The results of the compaction on silts and clays are conventionally presented in the form of a compaction curve. Figure 2 shows the relationship between moisture content, dry density, and average CT numbers for soil A. These results show a direct relationship between CT numbers and dry density and moisture content variation. Similar observations were reported by Tollner (1994). In addition to the compaction curve, the CT offers the possibility of studying the changes in the microstructure along chosen slices as well as three dimensionally. Figures 3 through 10 show a digital photograph, a radiograph of the specimen, a 3-D reconstructed image of the soil matrix and nine reconstructed slices of each specimen of soil A.

Compaction curve for soil A shows that the optimum moisture content is about 17% and maximum dry density is about 1740 kg/m^3. Specimens 1A and 2A have less moisture content than the optimum moisture content, whereas specimens 3A and 4A have a higher value.

The radiograph image of specimen 1A with the lowest moisture content (12.6%) shows a clear evidence of the boundaries of the five layers of compaction (Figure 3-b). The slice images provided by CT show the presence of

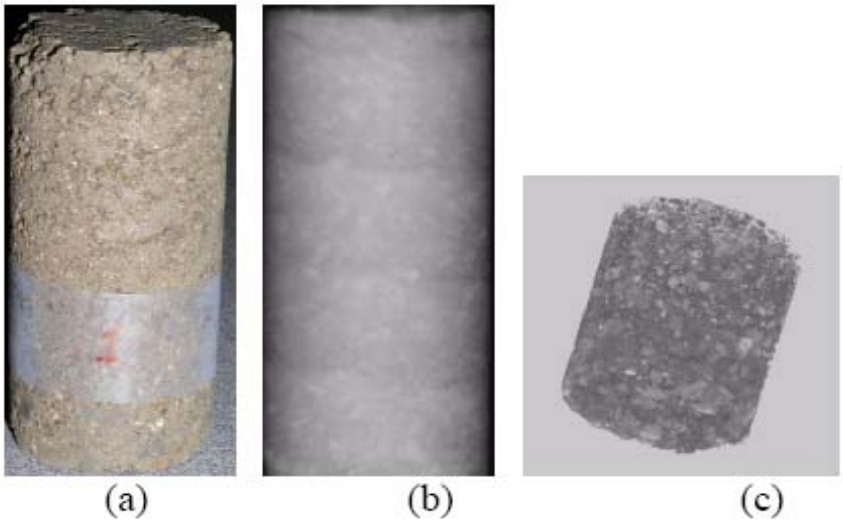

Figure (3) Specimen 1A; (a) digital photograph, (b) radiograph, (c) 3-D CT image.

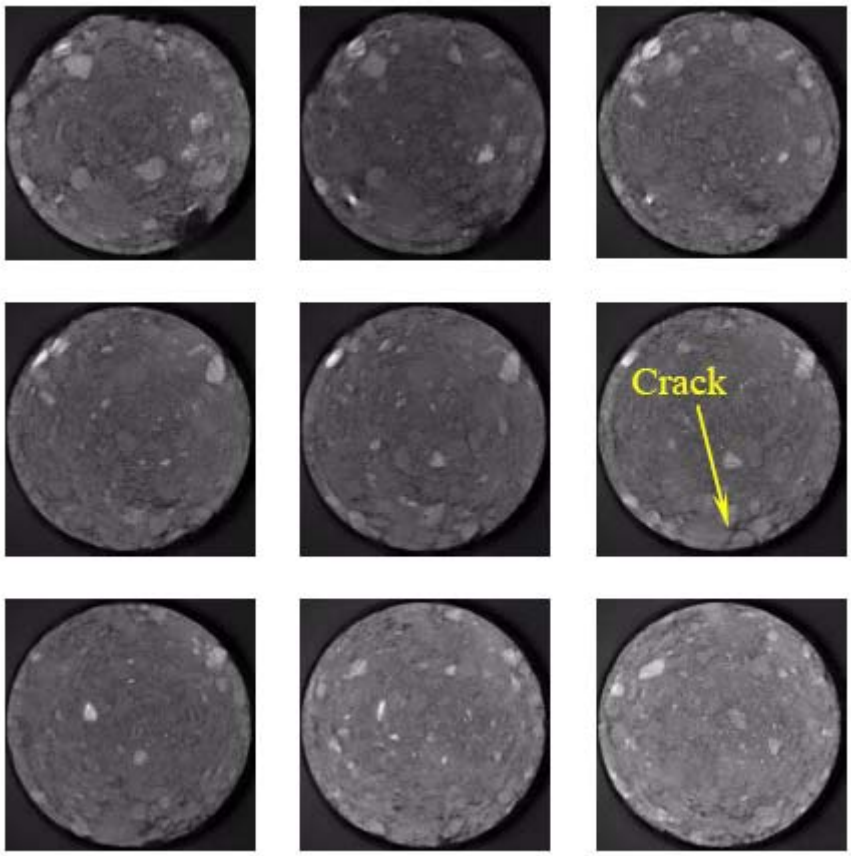

Figure (4): Representation of CT slices from middle height for Specimen 1A.

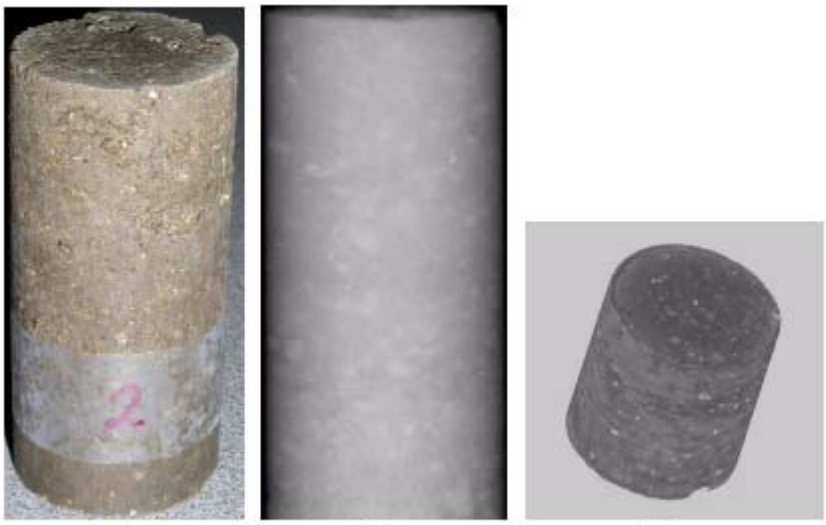

Figure (5): Specimen 2A; (a) digital photograph, (b) radiograph, (c) 3-D CT Image.

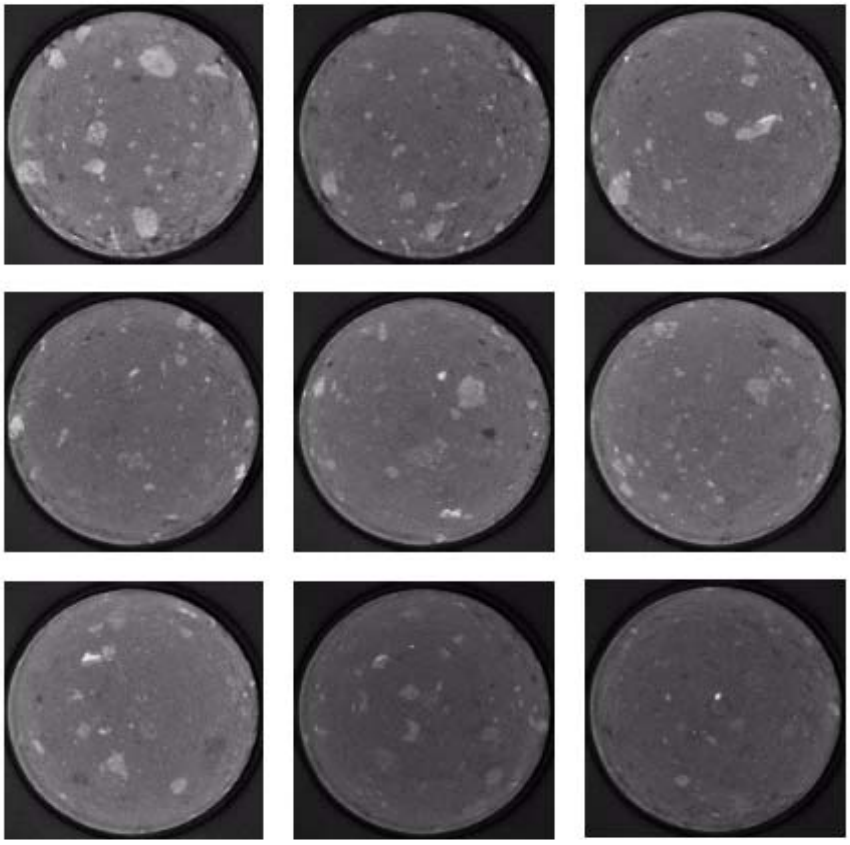

Figure (6): Representation of CT slices from middle height for Specimen 2A.

solids and voids. It can be seen that there is a large number of randomly scattered voids. The slices (Figure 4) as well as the 3-D radiograph (Figure 2-c) show the presence of cracks at various locations. When the water content is higher and near optimum (as in specimen 2A), there is little indication of the presence of boundaries between compacted layers (Figure 4-b). In addition, as expected, the number of voids is reduced and the CT slices look more uniform than in specimen 1A (Figures 4 and 5).

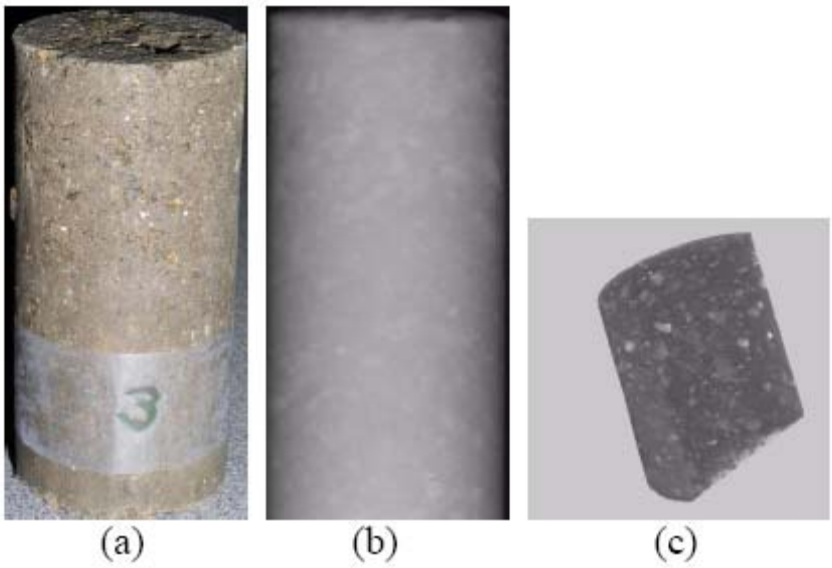

Figure (7): Specimen 3A; (a) digital photograph, (b) radiograph, (c) 3-D CT image.

The uniformity of the CT slices of specimen 3A with higher than optimum water content appears to be better than that of specimen 2A (Figure 7). Note that the density and the average values of CT numbers of both specimens are nearly the same. The three-dimensional soil matrix of specimen 4A (Figure 9-c) at a much higher water content than optimum is very similar to that of specimen 1A. The CT slices, however, appear to be more uniform in specimen 4A (Figure 10). This confirms that water replaces the pores and leads to a dispersion of the soil particles from optimum level as hypothesized by Lambe (1958).

The characteristics of the compaction and CT numbers of soil B essentially follow the patterns observed in soil A (Figure 11). Figures 12 through 15 show a 3-D CT image, a vertical section and a horizontal section of each specimen of soil B. The characteristics of these images also follow the pattern observed in soil A.

Soil C is sand, and it is known that shallow compaction does not lead to much changes in density. Therefore, in order to identify the variation of structure, the soil was tested at its minimum and maximum density conditions. Figures 16 and 17 show a 3-D CT image, a vertical section and a horizontal section of soil C for the minimum (specimen 1C) and maximum (specimen 2C) dry densities. It can be seen that the average CT numbers are higher for the specimen with maximum dry density. Moreover, in the specimen with minimum dry density pores are more and grains are visible very well (Figures 16 and 17). Slices of CT images of the maximum dry density look to be more uniform with less fluctuation in the density profile (Figure 17-c).

The CT images can also be used to characterize the orientation of particles and voids and their evolution with compaction using other software such as Matlab. This is currently under investigation. Finally, it is noted that the shear planes (pan caking) observed in the specimens of compacted soil confirm with McDonald's (1988) observations.

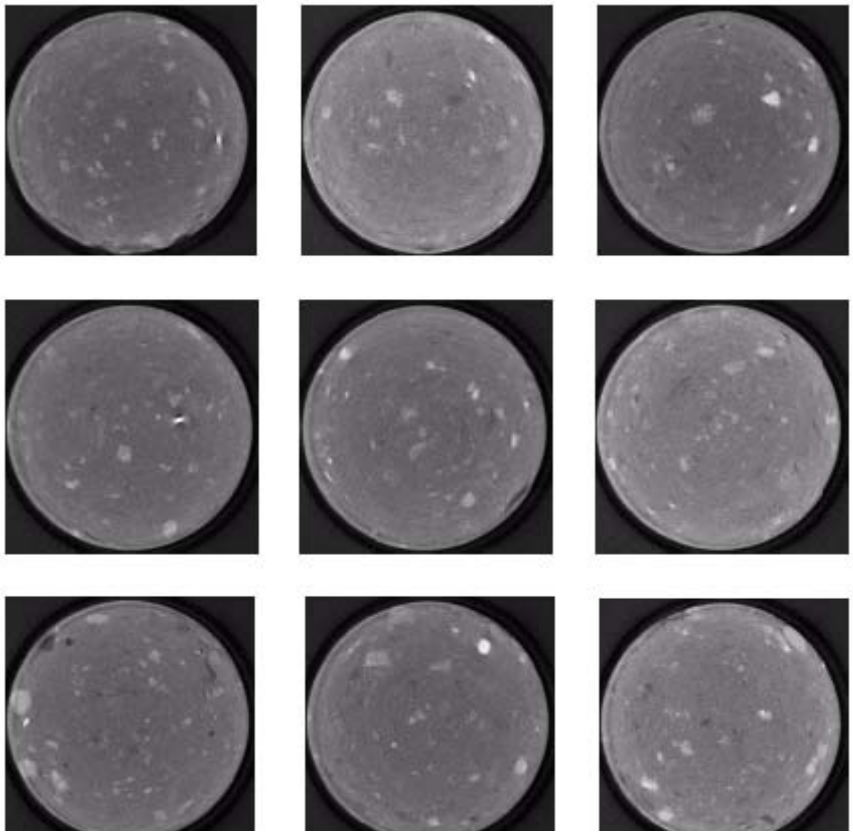

Figure (8): Representation of CT slices from middle height for specimen 3A.

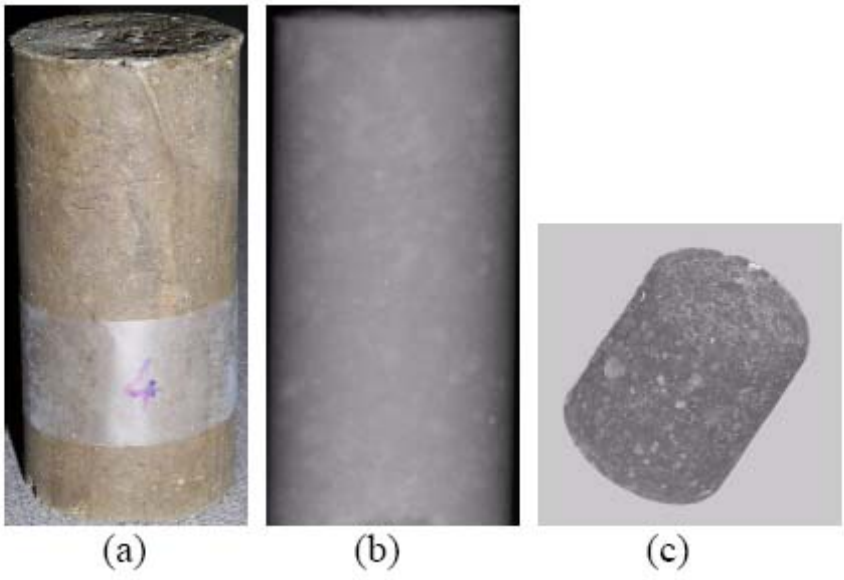

Figure (9): Specimen 4A; (a) digital photograph, (b) radiograph, (c) 3-D CT image.

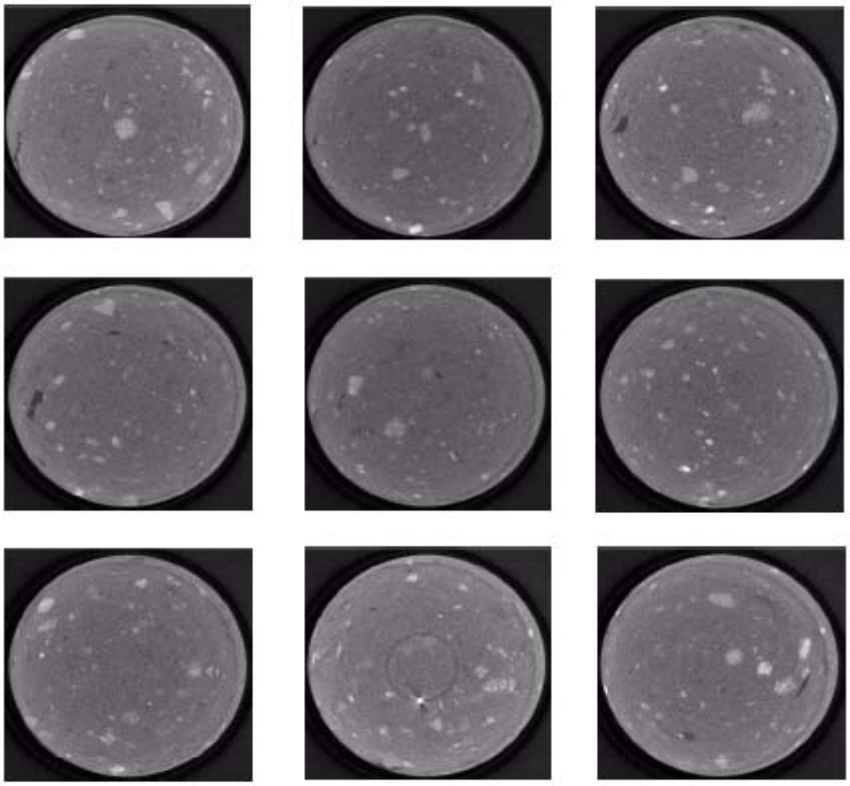

Figure (10): Representation of CT slices from middle height for specimen 4A.

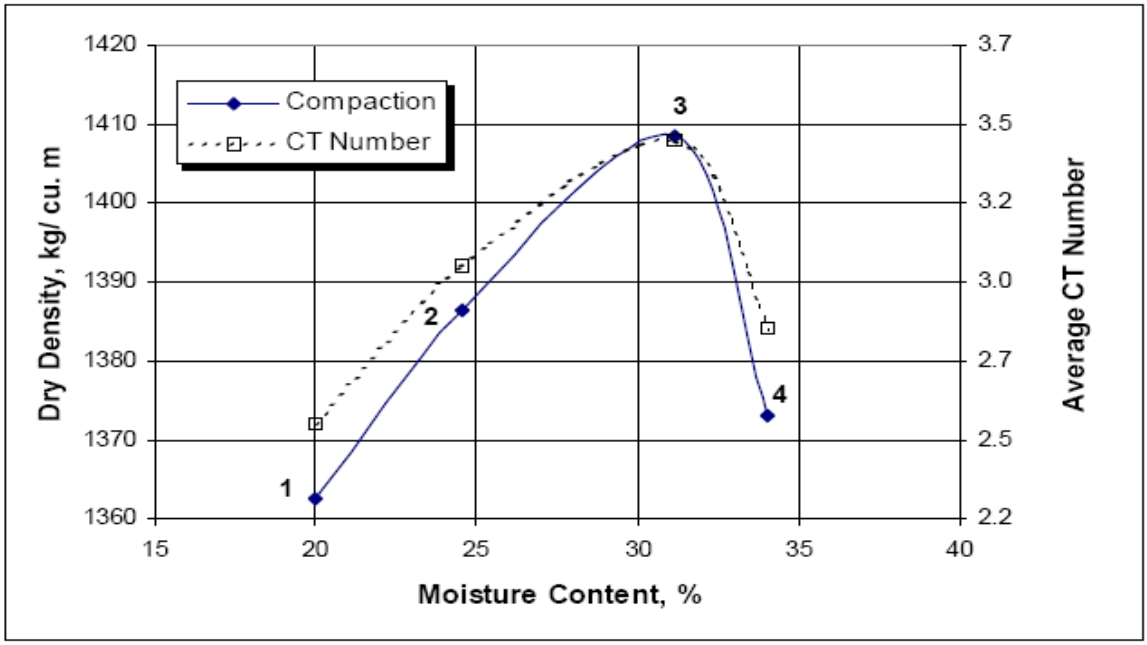

Figure (11): Compaction curve and CT numbers (soil B).

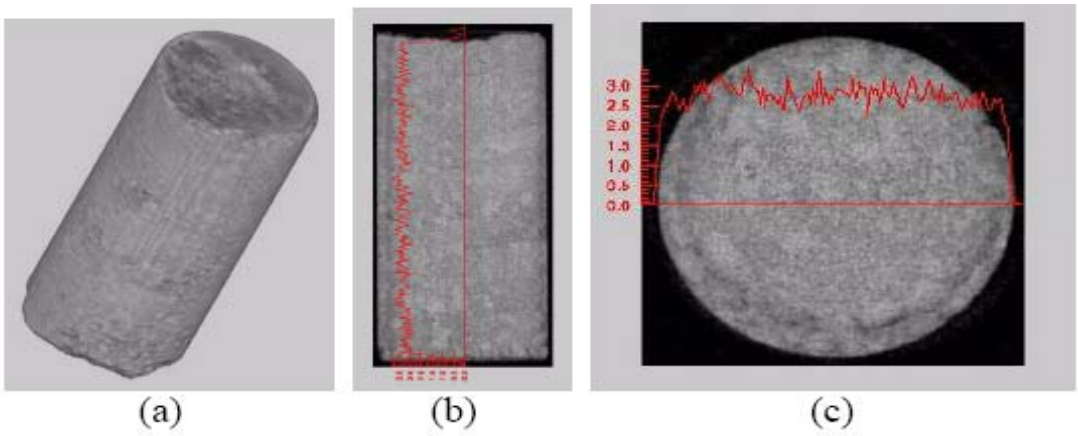

Figure (12): Specimen 1B; (a) 3-D CT image, (b) vertical slice, (c) horizontal slice.

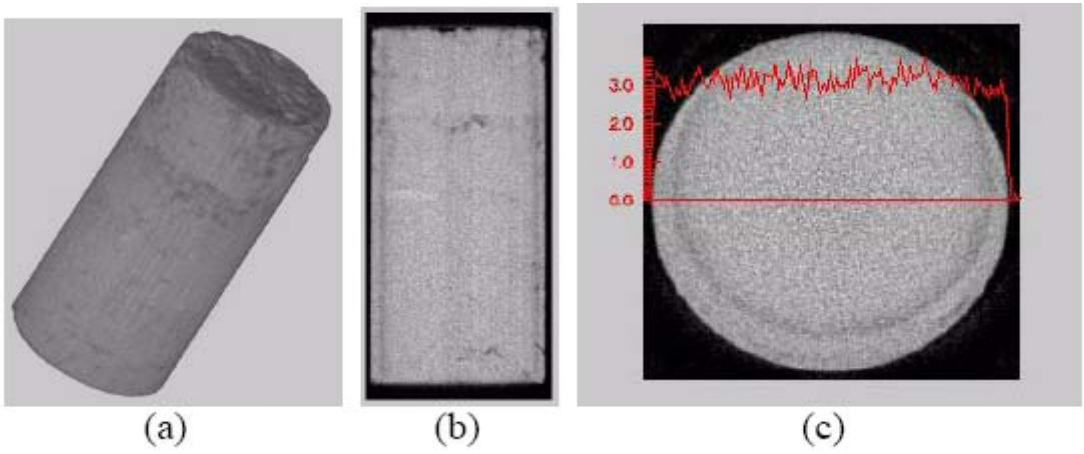

Figure (13): Specimen 2B; (a) 3-D CT image, (b) vertical slice, (c) horizontal slice.

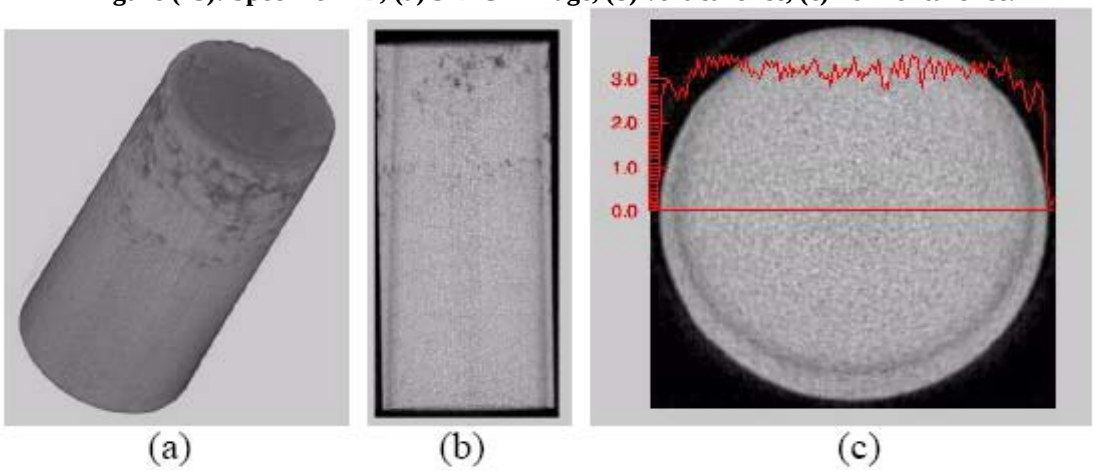

Figure (14): Specimen 3B; (a) 3-D CT image, (b) vertical slice, (c) horizontal slice.

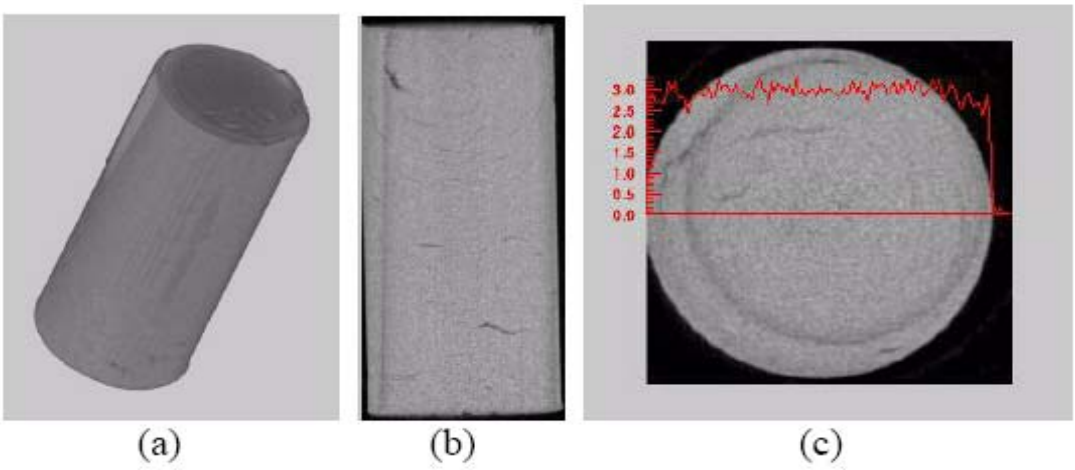

Figure (15): Specimen 4B; (a) 3-D CT image, (b) vertical slice, (c) horizontal slice.

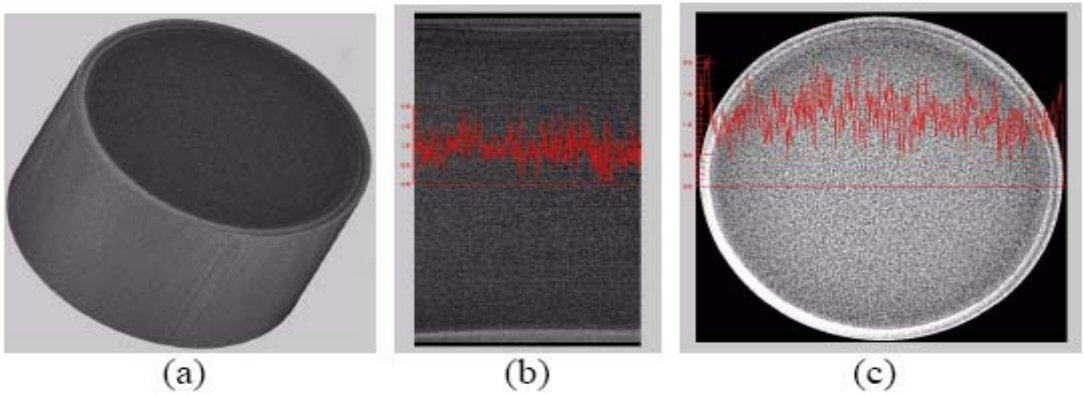

Figure (16): Specimen 1C with a minimum dry density; (a) 3-D CT image, (b) vertical slice, (c) horizontal slice.

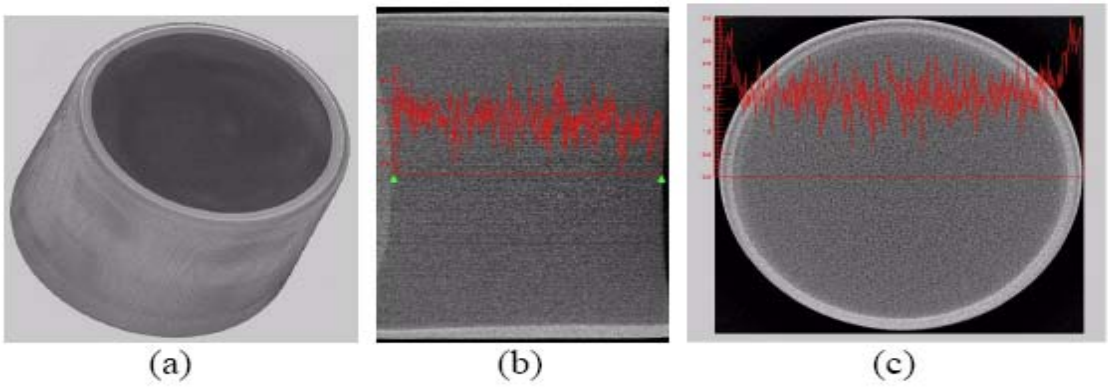

Figure (17): Specimen 2C with a maximum dry density; (a) 3-D CT image, (b) vertical slice, (c) horizontal slice.

CONCLUSIONS

This study presents a systematic method to examine the evolution of compaction curve using X-ray computed tomography images. It has been found that the relationship between average CT number and moisture content of the soil is similar to that shown in the compaction curve, and it has a maximum value at a moisture content very close to the optimum water content. Furthermore, studying the soil specimens beyond the optimum moisture content reveals a decrease in the amount of connected voids filled with air; consequently, air permeability decreases dramatically and cracks are developed as a result.

Finally, using X-ray computed tomography, the shear and weak planes can be identified. Therefore, it may be used as a powerful tool to quantify compaction of soils and other construction materials in dams and pavements in cases of serious predicaments.

REFERENCES

American Society for Testing and Materials. 2004. *Standard Guide for Evaluating Effectiveness of Chemicals for Soil Stabilization*, ASTM, Designation: D 4609-01, Annual Book of ASTM Standards, Philadelphia, PA.

American Society for Testing and Materials. 2003. *Standard Test Method for Calibrating and Measuring CT Density*, ASTM, Designation: D 1935 -97, Annual Book of ASTM Standards, Philadelphia, PA.

Bresson, L.M. and Moran, C.J. 1998. High-Resolution Bulk Density Images Using Calibrated X-Ray Radiography of Impregnated Soil Slices. *Soil Science Society of America J*., 62 (2): 299-304.

Buchanan, S.J. 1942. Soil Compaction. *Proc. 5th Texas Conf. Soil Mech*.

Hausmann, M.R. 1990. Engineering Principles of Ground Modification. McGraw-Hill Publishing Company.

Hilf, J.W. 1956. An Investigation of Pore-Water Pressure in Compacted Cohesive Soils. *Tech. Memo. 654*, US Department of the Interior, Bureau of Reclamation, Denver, Colorado.

Hogentogler, C.A. Jr. 1936. Essentials of Soil Compaction. *Proc. HRB.* 16: 209-216.

Ingles, O.G. and Metcalf, J.B. 1973. Soil Stabilization. John Wiley and Sons.

Rowe, K. 2000. Geotechnical and Geoenvironmental Engineering Handbook. Kluwer Academic Publishers.

Lambe, T.W. 1958. The Structure of the Compacted Clay, *Journal of the Soil Mechanics and Foundation Division*, ASCE 84, No. SM2, 1655-1 to 1655-35.

Leflaive, E. and Schaeffner, M. 1980. Compactibility of Soils Evaluated by the Measurement of Their Air Permeability. *Proc. ICC.*, I. 57-62.

McDonald, J.K. 1988. Discussion of the Paper by Sherard, Dunnigam and Talbot (1984). *J. Geotech. Eng. Div*., ASCE, 114 (2): 226-227.

Olson, R.E. 1963. Effective Stress Theory of Soil Compaction. *J. Soil Mech. Found. Div.*, ASCE, 89, No. SM2, 27-45.

Petrovic, A.M., Siebert, J.E. and Rieke, P.E. 1982. Soil Bulk Density Analysis in Three Dimensions by Computed Tomographic Scanning. *Soil Science Society of America J.*, 46 (3): 445-450.

Proctor, R.R. 1933. Design and Construction of Rolled Earth Dams. *Eng. News Record*, Aug. 31, Sept. 7, Sept. 21, Sept. 28, 245-248, 286-289, 341- 351 and 372-376, respectively.

Rogasic, H., Crawford, J.W., Wendroth, O., Young, I.M., Joschko, M. and Ritz, K. 1999. Discrimination of Soil Phases by Dual Energy X-ray Tomography, *Soil Science Society of America J*., 63: 741-751.

Seltzer, S.M. and Hubbell, J.H. 1995. Tables and Graphs of Photon Mass Attenuation Coefficient and Mass Energy-Absorption Coefficients for Photon Energies 1 keV to 20 MeV for Elements Z = 1 to 92 and Some Dosimetric Materials, Appendix to Invited Plenary Lecture by J.H. Hubbell "45 Years (1950-1995) with X-Ray Interactions

and Applications", Presented at the 51st National Meeting of the Japanese Society of Radiological Technology, April 14-16, 1995, Nagoya, Japan. *http:// physics.nist.gov/PhysRefData/ XrayMassCoef/ref.html*

Sherard, J.L., Dunnigan, L.P. and Talbot, J.R. 1984. Filters for Silts and Clays. *J. Geotech. Eng. Div*., ASCE, 110 (6): 701-718.

Tollner, E.W. 1994. Measurement of Density and Water Content in Soils with X-Ray Linescan and X-Ray Computed Tomography. *Transactions of the ASAE*, 37 (6): 1941-1948.

Whyte, I.L. and Vakalis, I.G. 1987. Shear Surfaces Induced in Clay Fills by Compaction Plant. in *Compaction Technology*, Thomas Telford, London, 125-137.